

Interpretable Outcome Prediction with Sparse Bayesian Neural Networks in Intensive Care

Hiske Overweg^{1*}, Anna-Lena Popkes^{1*}, Ari Ercole², Yingzhen Li^{1†},
José Miguel Hernández-Lobato^{1,2,3†}, Yordan Zaykov^{1†}, Cheng Zhang^{1†‡}
¹Microsoft Research Cambridge, UK, ² University of Cambridge, UK, ³ Alan Turing Institute, UK

Abstract

Clinical decision making is challenging because of pathological complexity, as well as large amounts of heterogeneous data generated as part of routine clinical care. In recent years, machine learning tools have been developed to aid this process. Intensive care unit (ICU) admissions represent the most data dense and time-critical patient care episodes. In this context, prediction models may help clinicians determine which patients are most at risk and prioritize care. However, flexible tools such as artificial neural networks (ANNs) suffer from a lack of interpretability limiting their acceptability to clinicians. In this work, we propose a novel interpretable Bayesian neural network architecture which offers both the flexibility of ANNs and interpretability in terms of feature selection. In particular, we employ a sparsity inducing prior distribution in a tied manner to learn which features are important for outcome prediction. We evaluate our approach on the task of mortality prediction using two real-world ICU cohorts. In collaboration with clinicians we found that, in addition to the predicted outcome results, our approach can provide novel insights into the importance of different clinical measurements. This suggests that our model can support medical experts in their decision making process.

Introduction

Clinicians often need to make critical decisions, for example, about treatments or patient scheduling, based on available data and personal expertise. The increasing prevalence of electronic health records (EHRs) means that routinely collected medical data are increasingly available in machine readable form. In some areas such as the intensive care unit (ICU), the data density may be so large that it becomes difficult for clinicians to fully appreciate relationships and patterns in clinical records. At the same time, ICU patients are the most severely ill. Life-supporting treatments are not only expensive and limited but may be associated with potentially catastrophic side effects. It is in this context that appropriate treatments must be delivered in a time-critical

manner based on accurate appraisal of all available information. A degree of automated data analysis may assist clinicians navigate the current ‘data deluge’ and make the best informed decisions. The recent success of artificial intelligence and machine learning in various real-world applications suggests that such technology can be the key to unlocking the full potential of medical data and help with making real-time decisions (Shipp et al. 2002; Caruana et al. 2015; Bouton et al. 2016; Chen et al. 2017).

The high data density of the ICU is ideal for applying machine learning methods to assist with clinical decision making. All medical decision making is predicated on the prediction of future outcomes. Especially relevant to the ICU are predictions surrounding patient mortality. As a consequence, several machine learning studies published over the course of the last years focused on this task (Joshi and Szolovits 2012; Celi et al. 2012; Ghassemi et al. 2014; Meiring et al. 2018). Most of these studies concentrated on improving previously published measures of performance such as discrimination, specificity and sensitivity.

Deploying machine learning solutions in ICUs to support life/death decision making is challenging and requires high prediction accuracy. Artificial neural networks (ANNs) are powerful machine learning models that have been successful in several highly complex real-world tasks (Collobert et al. 2011; Boulanger-Lewandowski, Bengio, and Vincent 2012; Bojarski et al. 2016; Silver et al. 2016). The non-linearity of ANNs allows them to capture complex non-linear dependencies, a quality which often results in high predictive performance. Despite widespread success, predictions from ANNs lack interpretability. Instead, they often function as a black box. For example, after training an ANN on the task of outcome prediction it is difficult to determine which input features are relevant for making predictions. This is highly undesirable in the medical domain — making potentially life-changing decisions without being able to clearly justify them is unacceptable to both clinicians and patients. As a consequence, the application of ANNs in practice has been limited. Advancing the interpretability of such networks is essential to increase their impact in healthcare applications.

In this work, we propose an interpretable machine learning model based on a Bayesian neural network (BNN)

*Equal contribution. Performed during the authors’ involvement in the Microsoft AI Residency Program.

†Equal contribution from senior authors

‡Corresponding author: Cheng.Zhang@microsoft.com
2019

(MacKay 1992; Hinton and Van Camp 1993; Blundell et al. 2015; Hernández-Lobato and Adams 2015; Louizos, Ullrich, and Welling 2017; Ghosh and Doshi-Velez 2017) for outcome prediction in the ICU. Our proposed method offers not only the flexibility of ANNs but also interpretable predictions — inspecting the model parameters directly shows which features are considered irrelevant for prediction. In particular, we propose the use of tied sparsity inducing prior distributions, where the same sparsity prior is shared among all weights connected to the same input feature. For some of the input features, all of their connecting weights will be suppressed after training, indicating that the corresponding input features are not relevant for prediction. For the prior distribution we use the horseshoe prior because of its sparsity inducing and heavy-tailed nature. Furthermore a BNN explicitly models the uncertainty in a dataset, as well as in the model parameters and predictions. This replicates the inherently probabilistic nature of clinical decision making.

We apply our method to two real-world ICU cohorts, MIMIC-III (Johnson et al. 2016) and CENTER-TBI (Maas et al. 2014), to predict patient outcome. The model provides fully probabilistic predictions. Such results can help clinicians with making treatment decisions and communicating with patients’ families. More importantly, our method allows to determine which medical measures are irrelevant for the task of outcome prediction. This is an important advance because model interpretability is essential if critical decisions based on diagnostic support systems are to be accepted by both clinicians and the public.

Related work

Sparsity in linear models In linear models sparsity is typically induced using a suitable prior distribution over the model parameters. The well known LASSO (Least Absolute Shrinkage and Selection Operator) (Tibshirani 1996) produces a sparse estimate of the parameters in a linear model, by regularizing the ℓ_1 norm of the parameter vector. Park and Casella (2008) showed that the ℓ_1 regularizer can be interpreted as a Laplace prior over the parameters, and that the LASSO estimate is equivalent to a maximum a posteriori estimate of the linear coefficients given data.

Sparsity inducing prior distributions beyond the Laplace distribution have been proposed to improve feature selection results. For example, the spike and slab prior places a mixture distribution on each parameter, comprising a point mass distribution at zero (the spike) and an absolutely continuous density (the slab) (Mitchell and Beauchamp 1988).

The spike and slab prior requires a careful choice of the mixture weights and the variance of the “slab”. Another popular choice for introducing sparsity is the horseshoe prior (Carvalho, Polson, and Scott 2009), which assigns a half-Cauchy prior over the variance of the Gaussian prior over the parameters. The heavy tail of the horseshoe distribution allows coefficients associated with important features to remain large, while at the same time the tall spike at the origin encourages shrinkage of other parameters. Compared to the spike and slab prior, the horseshoe prior is more stable and more computationally efficient. Therefore, in this work we

employ the horseshoe prior as the sparsity inducing prior for feature selection.

Sparsity in non-linear models Less work has been directed towards the application of sparsity inducing priors in non-linear models. One of the first approaches was Automatic Relevance Determination applied to BNNs (MacKay and others 1994), which fits the prior variance for each individual parameters by maximizing the marginal likelihood. However, this approach fails to scale to large datasets as it involves the inversion of large matrices. Louizos, Ullrich, and Welling (2017) and Ghosh and Doshi-Velez (2017) applied a horseshoe prior to prune inactive hidden units from BNNs, thereby achieving better compression. Our work uses the same inference techniques, however, we focus on selecting input features, not hidden units.

Outcome prediction in the medical domain Because of its central importance to patients and clinicians, outcome prediction for ICU patients is a widely studied task. Models can be divided into two categories: those using only static features (Knaus et al. 1985; Le Gall, Lemeshow, and Saulnier 1993; Lemeshow et al. 1993; Elixhauser et al. 1998; Steyerberg et al. 2008) and those utilizing information about the temporal evolution of features (Joshi and Szolovits 2012; Ghassemi et al. 2014; Caballero B. and Akella 2015; Harutyunyan et al. 2017; Che et al. 2018).

Most approaches based on static features model only *linear* relationships or rely on manual feature engineering. Manual feature engineering scales poorly, and prevents models from automatically discovering patterns in the data. Linear models are easy to interpret, because the importance of input features can directly be inferred from the magnitude of the associated model coefficients. This is highly desirable for transparent clinical decision making, but the capacity of linear models is limited. In most real world problems the relationship between input features and target values is *non-linear* or may involve complex interactions between predictors. Consequently, more powerful approaches are required.

In this work, we propose a model for mortality prediction named HorseshoeBNN. In contrast to previous work (Joshi and Szolovits 2012; Celi et al. 2012; Ghassemi et al. 2014; Caballero B. and Akella 2015) our model is able to both capture non-linear relationships and learn which input features are important for prediction.

Methods

In this section, we describe our proposed BNN architecture for mortality prediction. We first revisit the BNN, a type of ANN which explicitly models uncertainty by introducing distributions over the model parameters. We then introduce the specific prior distribution we employ, the horseshoe prior, which induces sparsity in the first layer of the BNN, thereby enabling features selection. Finally we describe the architecture of our model, the HorseshoeBNN, and discuss the computational methods to implement it.

Bayesian Neural Networks

Given an observed dataset $\mathcal{D} = \{(\mathbf{x}_n, \mathbf{y}_n)\}_{n=1}^N$, an ANN uses a set of parameters θ to determine a model $\mathbf{y} = f(\mathbf{x}; \theta)$ that fits the data well and generalizes to unseen cases. Instead of directly predicting the response \mathbf{y} with a deterministic function f , BNNs start from a probabilistic description of the modelling task, and estimate the uncertainty of the parameters given the data. Concretely, the network parameters θ are considered random variables, and a prior distribution $p(\theta)$ is selected to represent the prior belief of their configuration. Assuming that the observed data is independent and identically distributed (i.i.d.), the *likelihood function* of θ is defined as

$$p(\mathcal{D}|\theta) = \prod_{n=1}^N p(\mathbf{y}_n|\mathbf{x}_n, \theta), \quad (1)$$

where, in case of a binary classification task like the one presented in this work, the label y_n is a scalar, and

$$\log p(y_n|\mathbf{x}_n, \theta) = y_n \log(f(\mathbf{x}_n); \theta) + (1 - y_n) \log(1 - f(\mathbf{x}_n; \theta)). \quad (2)$$

For regression tasks, we have $p(\mathbf{y}_n|\mathbf{x}_n, \theta) = \mathcal{N}(\mathbf{y}_n; f(\mathbf{x}_n; \theta), \sigma^2 \mathbf{I})$. After observing the training data \mathcal{D} , a *posterior distribution* of the network weights θ is defined by Bayes' rule

$$p(\theta|\mathcal{D}) = \frac{p(\theta)p(\mathcal{D}|\theta)}{p(\mathcal{D})}, \quad p(\mathcal{D}) = \int p(\theta)p(\mathcal{D}|\theta)d\theta. \quad (3)$$

This posterior distribution represents the *updated* belief of how likely the network parameters are given the observations. It can be used to predict the response \mathbf{y}^* of an unseen input \mathbf{x}^* using the *predictive distribution*:

$$p(\mathbf{y}^*|\mathbf{x}^*, \mathcal{D}) = \int p(\mathbf{y}^*|\mathbf{x}^*, \theta)p(\theta|\mathcal{D})d\theta. \quad (4)$$

The HorseshoeBNN: Feature Selection with Sparsity Inducing Priors

The prior distribution $p(\theta)$ captures the prior belief about which model parameters are likely to generate the target outputs \mathbf{y} , before observing any data. When focusing on feature selection, sparsity inducing priors are of particular interest. In this work, we use a horseshoe prior (Carvalho, Polson, and Scott 2009), which can be described as

$$w|\tau \sim \mathcal{N}(0, \tau^2) \quad \text{where} \quad \tau \sim C^+(0, b_0), \quad (5)$$

where C^+ is the half-Cauchy distribution and τ is a scale parameter. The probability density function of the horseshoe prior with $b_0 = 1$ is illustrated in Figure 1. It has a sharp peak around zero and wide tails. This encourages shrinkage of weights that do not contribute to prediction, while at the same time allowing large weights to remain large.

For feature selection we propose a horseshoe prior for the first layer of a BNN by using a shared half-Cauchy distribution to control the shrinkage of weights connected to the same input feature. Specifically, denoting $W_{ij}^{(1)}$ as the weight connecting the j -th component of the input vector

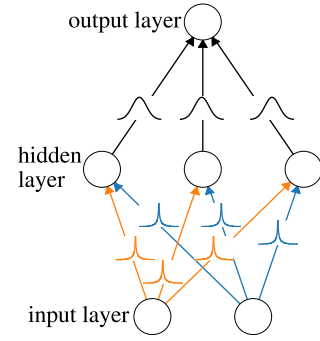


Figure 1: Illustration of a HorseshoeBNN. The prior distribution of the weights in the input layer is given by a horseshoe distribution. All weights for particular input feature share the same shrinkage parameter, allowing for feature selection. The prior of the weights of the second layer is given by a Gaussian.

\mathbf{x} to the i -th node in the first hidden layer, the associated horseshoe prior is given by

$$W_{ij}^{(1)}|\tau_n, v \sim \mathcal{N}(0, \tau_j^2 v^2) \quad (6)$$

where $\tau_j \sim C^+(0, b_0)$ and $v \sim C^+(0, b_g)$.

The layer-wide scale v tends to shrink all weights in a layer, whereas the local shrinkage parameter τ_j allows for reduced shrinkage of all weights related to a specific input feature x_j . As a consequence, certain features of the input vector \mathbf{x} are selected whereas others are ignored. For the bias node we use a Gaussian prior distribution. It is important to note that a simpler solution which keeps all feature weights small but does not encourage significant shrinkage would not be sufficient for feature selection — large weights in deeper layers of the network might increase the influence of irrelevant input features.

We model the prior of the weights in the second layer of the HorseshoeBNN by a Gaussian distribution, which prevents overfitting (Blundell et al. 2015). The complete network architecture is given in Figure 1. Although we perform our experiments with a single hidden layer, the model can easily be enlarged by adding more hidden layers with Gaussian priors.

A direct parameterization of the half-Cauchy prior can lead to instabilities in variational inference (VI) for BNNs. Thus, we follow Ghosh and Doshi-Velez (2017) to reparametrize the horseshoe prior using auxiliary parameters:

$$\begin{aligned} a \sim C^+(0, b) &\Leftrightarrow \\ a|\kappa &\sim \text{Inv} \Gamma\left(\frac{1}{2}, \frac{1}{\kappa}\right); \quad \kappa \sim \text{Inv} \Gamma\left(\frac{1}{2}, \frac{1}{b^2}\right). \end{aligned} \quad (7)$$

After adding the auxiliary variables to the Horseshoe prior, the prior over all the unobserved random variables $\theta = \{\{\mathbf{W}^{(l)}\}_{l=1}^{L+1}, v, \vartheta, \boldsymbol{\tau} = \{\tau_j\}, \boldsymbol{\lambda} = \{\lambda_j\}\}$ is

$$p(\theta) = p(\mathbf{W}^{(1)}, v, \vartheta, \boldsymbol{\tau}, \boldsymbol{\lambda}) \prod_{l=2}^{L+1} p(\mathbf{W}^{(l)}),$$

$$\begin{aligned}
p(\mathbf{W}^{(l)}) &= \prod_{i,j} \mathcal{N}(W_{ij}^{(l)}; 0, \sigma^2), \quad l = 2, \dots, L+1, \\
p(\mathbf{W}^{(1)}, v, \vartheta, \boldsymbol{\tau}, \boldsymbol{\lambda}) &= \\
p(v|\vartheta) p(\vartheta) \prod_j p(\tau_j|\lambda_j) p(\lambda_j) \prod_i \mathcal{N}(W_{ij}^{(1)}; 0, \tau_j^2 v^2), \\
p(\tau_j|\lambda_j) &= \text{Inv } \Gamma\left(\frac{1}{2}, \frac{1}{\lambda_j}\right), \quad p(\lambda_j) = \text{Inv } \Gamma\left(\frac{1}{2}, \frac{1}{b_0^2}\right), \quad (8) \\
p(v|\vartheta) &= \text{Inv } \Gamma\left(\frac{1}{2}, \frac{1}{\vartheta}\right), \quad p(\vartheta) = \text{Inv } \Gamma\left(\frac{1}{2}, \frac{1}{b_0^2}\right).
\end{aligned}$$

Scalable Variational Inference for HorseshoeBNN

For most BNN architectures both the posterior distribution $p(\boldsymbol{\theta}|\mathcal{D})$ and the predictive distribution $p(\mathbf{y}^*|\mathbf{x}^*, \mathcal{D})$ are intractable due to a lack of analytic forms for the integrals. To address this outstanding issue we fit a simpler distribution $q_\phi(\boldsymbol{\theta}) \approx p(\boldsymbol{\theta}|\mathcal{D})$ and later replace $p(\boldsymbol{\theta}|\mathcal{D})$ with $q_\phi(\boldsymbol{\theta})$ in prediction. More specifically, we define

$$\begin{aligned}
q_\phi(\boldsymbol{\theta}) &= q_\phi(\mathbf{W}^{(1)}|\boldsymbol{\tau}, v) q_\phi(v) q_\phi(\vartheta) q_\phi(\boldsymbol{\tau}) q_\phi(\boldsymbol{\lambda}) \\
&\times \prod_{l=2}^{L+1} q_\phi(\mathbf{W}^{(l)}), \quad (9)
\end{aligned}$$

and use factorized Gaussian distributions for the weights in upper layers:

$$q(\mathbf{W}^{(l)}) = \prod_{i,j} \mathcal{N}(W_{ij}^{(l)}|\mu_{W_{ij}^{(l)}}, \sigma_{W_{ij}^{(l)}}^2), \quad l = 2, \dots, L+1.$$

To ensure non-negativity of the shrinkage parameters, we consider a log-normal approximation to the posterior of v and τ_j , i.e.

$$q_\phi(v) = \mathcal{N}(\log v; \mu_v, \sigma_v^2), \quad q_\phi(\tau_j) = \mathcal{N}(\log \tau_j; \mu_{\tau_j}, \sigma_{\tau_j}^2). \quad (10)$$

In the horseshoe prior (see Eq. 5) the weights W_{ij} and the scales τ_l and v are strongly correlated. This leads to strong correlations in the posterior distribution with pathological geometries that are hard to approximate. Betancourt and Girolami (2015) and Ingraham and Marks (2016) show that this problem can be mitigated by reparametrizing the weights in the horseshoe layer as follows:

$$\beta_{ij} \sim \mathcal{N}(\beta_{ij}|\mu_{\beta_{ij}}, \sigma_{\beta_{ij}}^2), \quad W_{ij}^{(1)} = \tau_l v \beta_{ij}, \quad (11)$$

and equivalently, parametrizing the approximate distribution $q(\mathbf{W}^{(1)}|v, \boldsymbol{\tau})$ as

$$\begin{aligned}
q(\mathbf{W}^{(1)}|v, \boldsymbol{\tau}) &= \prod_{i,j} q(W_{ij}^{(1)}|v, \tau_j) \\
&= \prod_{i,j} \mathcal{N}(W_{ij}^{(1)}; v\tau_j\mu_{\beta_{ij}}, v^2\tau_j^2\sigma_{\beta_{ij}}^2). \quad (12)
\end{aligned}$$

Because the log-likelihood term $p(\mathbf{y}|\mathbf{x}, \boldsymbol{\theta})$ does not depend on ϑ or $\boldsymbol{\lambda}$, one can show that the optimal approximations $q(\vartheta)$ and $q(\boldsymbol{\lambda})$ are inverse Gamma distributions with distributional parameters dependent on $q(\boldsymbol{\theta} \setminus \{\vartheta, \boldsymbol{\lambda}\})$ (Ghosh and Doshi-Velez 2017).

We fit the variational posterior $q_\phi(\boldsymbol{\theta})$ by minimizing the Kullback-Leibler (KL) divergence $\text{KL}[q_\phi(\boldsymbol{\theta})||p(\boldsymbol{\theta}|\mathcal{D})]$. One can show that the KL divergence minimization task is equivalent to maximizing the *evidence lower-bound* (ELBO) (Jordan et al. 1999; Beal 2003; Zhang et al. 2018)

$$\begin{aligned}
\mathcal{L}(\phi) &= \mathbb{E}_{q_\phi(\boldsymbol{\theta})} [\log p(\mathcal{D}|\boldsymbol{\theta})] - \text{KL}[q_\phi(\boldsymbol{\theta})||p(\boldsymbol{\theta})] \\
&= \mathbb{E}_{q_\phi(\boldsymbol{\theta})} [\log p(\mathcal{D})] - \text{KL}[q(\boldsymbol{\theta}|\phi)||p(\boldsymbol{\theta}|\mathcal{D})].
\end{aligned}$$

Since the ELBO still lacks an analytic form due to the non-linearity of the BNN, we apply black box VI (Ranganath, Gerrish, and Blei 2014) to compute an unbiased estimate of the ELBO by sampling $\boldsymbol{\theta} \sim q_\phi(\boldsymbol{\theta})$. More specifically, because the q distribution is constructed by a product of (log-) normal distributions, we apply the reparametrization trick (Kingma and Welling 2013; Rezende, Mohamed, and Wierstra 2014) to draw samples from the variational distribution: $w \sim \mathcal{N}(w; \mu, \sigma^2) \Leftrightarrow \epsilon \sim \mathcal{N}(\epsilon; 0, 1), w = \mu + \sigma\epsilon$. Furthermore, stochastic optimization techniques are employed to allow for mini-batch training, which enables the VI algorithm to scale to large datasets. Combining both, the *doubly stochastic* approximation to the ELBO is

$$\begin{aligned}
\mathcal{L}(\phi) &\approx \frac{N}{M} \sum_{m=1}^M \log p(\mathbf{y}_m|\mathbf{x}_m, \boldsymbol{\theta}) - \text{KL}[q_\phi(\boldsymbol{\theta})||p(\boldsymbol{\theta})], \\
\boldsymbol{\theta} &\sim q_\phi(\boldsymbol{\theta}), \quad \{(\mathbf{x}_m, \mathbf{y}_m)\}_{m=1}^M \sim \mathcal{D}^M,
\end{aligned}$$

which is used as the loss function for the stochastic gradient ascent training of the variational parameters ϕ .

Experiments and Results

We evaluate our model on several datasets. In Appendix A we present a validation study on a synthetic feature selection dataset, showing that our approach can recover the ground truth set of features. Here we present a performance benchmark on datasets from the UCI repository and then evaluate our method on two real-world ICU cohorts: MIMIC-III (Johnson et al. 2016) and CENTER-TBI (Maas et al. 2014).

Experimental Set-Up

We compare our proposed HorseshoeBNN with the following methods.

- *LinearGaussian*: a linear model with a Gaussian prior distribution on all weights (Bishop 2006). This is the most commonly used Bayesian model for prediction tasks.
- *GaussianBNN*: a standard BNN with a Gaussian prior distribution on all weights (Blundell et al. 2015).
- *LinearHorseshoe*: a linear model with a horseshoe prior distribution on all weights (Carvalho, Polson, and Scott 2009). This model uses sparsity inducing prior distributions for performing feature selection.
- *HorseshoeBNN*: our novel extension of the GaussianBNN with a tied horseshoe prior distribution on the weights in the first layer. This enables the model to perform feature selection.
- *Lasso*: For details, see Appendix B.
- *SupportVectorMachine* (SVM): see Appendix B.
- *RandomForest*: see Appendix B.

All models are trained until convergence using 10 fold cross-validation and the ADAM optimizer (Kingma and Ba 2014). We use 50 hidden units for the UCI datasets and MIMIC-III cohort and 100 hidden units for CENTER-TBI. The full list of hyperparameter settings can be found in Appendices C and D.¹

UCI benchmark

We report the root mean squared error (RMSE) and negative log-likelihood (NLL) results on three regression datasets from the UCI repository. The GaussianBNN and the Horseshoe BNN perform better than the linear models. The RandomForest performs best in terms of RMSE on these small datasets. However, it does not provide a principled probabilistic estimation and its performance is worse for the clinical datasets discussed below.

Dataset	Model	RMSE	NLL
Boston	LinearGaussian	4.806 ± 0.191	2.992 ± 0.039
	GaussianBNN	3.470 ± 0.283	2.646 ± 0.085
	LinearHorseshoe	4.840 ± 0.206	3.018 ± 0.038
	HorseshoeBNN	3.500 ± 0.243	2.617 ± 0.062
	Lasso	4.79 ± 0.19	-
	SVM	4.990 ± 0.254	-
	RandomForest	3.151 ± 0.145	-
Yacht	LinearGaussian	9.008 ± 0.366	3.627 ± 0.039
	GaussianBNN	1.157 ± 0.069	1.582 ± 0.030
	LinearHorseshoe	8.921 ± 0.367	3.616 ± 0.037
	HorseshoeBNN	0.959 ± 0.091	1.334 ± 0.139
	Lasso	8.95 ± 0.45	-
	SVM	10.715 ± 0.831	-
	RandomForest	0.989 ± 0.110	-
Wine	LinearGaussian	0.652 ± 0.013	0.993 ± 0.020
	GaussianBNN	0.640 ± 0.014	0.974 ± 0.019
	LinearHorseshoe	0.635 ± 0.013	0.966 ± 0.020
	HorseshoeBNN	0.639 ± 0.012	0.974 ± 0.016
	Lasso	0.652 ± 0.013	-
	SVM	0.654 ± 0.015	-
	RandomForest	0.570 ± 0.010	-

Table 1: Test performance in RMSE and negative log likelihood, the lower the better.

Mortality prediction on MIMIC-III

Cohort MIMIC-III (Medical Information Mart for Intensive Care) (Johnson et al. 2016) is a publicly available intensive care database collected from tertiary care hospitals. The data includes information about laboratory measurements, medications, notes from care providers and other features. In total, the database contains medical records of 7.5K ICU patients over 11 years.

Preprocessing We preprocess MIMIC-III using code introduced in Harutyunyan et al. (2017), focusing on the task of mortality prediction. For all measurements we remove invalid feature values beyond the allowed range defined by medical experts (see Table 7 in Appendix C). Since we do not focus on prediction based on dynamic features, we reduce the time series for each patient by computing the mean value of each feature in the first 48 hours of the patient’s

¹The code for the experiments is available at <https://github.com/microsoft/horseshoe-bnn>

stay in the ICU. We use mean imputation for missing values. The final cohort contains 17903 samples and 17 features. 86.5% of patients contained in the dataset survived, 13.5% deceased. All features are listed in Table 7 in Appendix C.

Prediction We present the error rate, the area under the receiver operating characteristic curve (AUROC) and negative predictive log-likelihood results in Table 2. Overall, the BNNs perform better than the other models. The HorseshoeBNN performs on par with or slightly better than the GaussianBNN, potentially because better feature selection reduces overfitting. We also present the confusion matrix for the Horseshoe models in Figure 3. Although the dataset is imbalanced with a significantly smaller amount of deceased patient data, the HorseshoeBNN still show an improvement in correctly predicting the outcome of deceased patients compared to the LinearHorseshoe model.

Interpretability and Clinical Relevance In addition to improved predictive performance, the HorseshoeBNN allows for better feature selection. For linear models we inspect the posterior mean of the weights directly connected to the features. For BNNs we look at the average of the posterior means of the outgoing weights. We plot a histogram of these weight values with logarithmic bins (see Appendix C). For the horseshoe models, the histogram shows two groups of weights which differ by orders of magnitude, facilitating the choice of a threshold for feature relevance. We verify that the metric values remain unchanged when training a horseshoeBNN without the features considered irrelevant by the model. The clear dichotomy in the histogram of the weights is absent for Gaussian models (see Appendix C), showing the importance of the horseshoe prior to efficiently eliminate irrelevant features.

The ability to perform feature selection also improves the interpretability of the model predictions. The weight values described above reflect the relevance of the features and are visualised in Figure 2. We find that the LinearHorseshoe model and the HorseshoeBNN agree on the relevance of most features except for *pH*, *systolic blood pressure* and *Glasgow coma scale*.

The HorseshoeBNN picks up the pH feature, whereas the LinearHorseshoe model does not, presumably because the outcome depends on pH values in a non-linear way (which a linear model cannot capture): the healthy range for pH is very narrow and both too high and too low values are dangerous.

For blood pressure, the LinearHorseshoe model captures the diastolic blood pressure only, while the HorseshoeBNN captures both the diastolic and systolic blood pressure. Although recording diastolic pressure is sufficient to establish a baseline blood pressure for a patient, combining diastolic and systolic values allows to obtain additional information about the waveform of a patient’s blood pressure, which can be of clinical relevance. This suggests that the HorseshoeBNN is able to recognize the importance of this extra information, whereas the LinearHorseshoe model is not.

The feature *Glasgow coma scale total* is selected only by

Model	Error rate	AUROC	NLL
LinearGaussian	0.129 ± 0.003	0.807 ± 0.004	0.321 ± 0.004
GaussianBNN	0.123 ± 0.003	0.830 ± 0.004	0.304 ± 0.004
LinearHorseshoe	0.130 ± 0.003	0.807 ± 0.004	0.320 ± 0.004
HorseshoeBNN	0.122 ± 0.002	0.831 ± 0.004	0.304 ± 0.004
Lasso	0.129 ± 0.002	0.795 ± 0.004	0.325 ± 0.004
SVM	0.129 ± 0.003	-	-
RandomForest	0.125 ± 0.002	-	-

Table 2: Results of the different models for the task of mortality prediction tested on the MIMIC-III cohort. NLL is the negative log-likelihood. The mean value and standard error of each metric over 10-fold cross-validation is presented.

		LinearHorseshoe		HorseshoeBNN	
True label	deceased	0.979	0.021	0.975	0.025
	survived	± 0.001	± 0.001	± 0.003	± 0.003
True label	deceased	0.825	0.175	0.743	0.257
	survived	± 0.008	± 0.008	± 0.018	± 0.018
		Predicted label		Predicted label	
		survived	deceased	survived	deceased

Table 3: Confusion matrices of the horseshoe models trained on the MIMIC-III cohort (10-fold cross-validated).

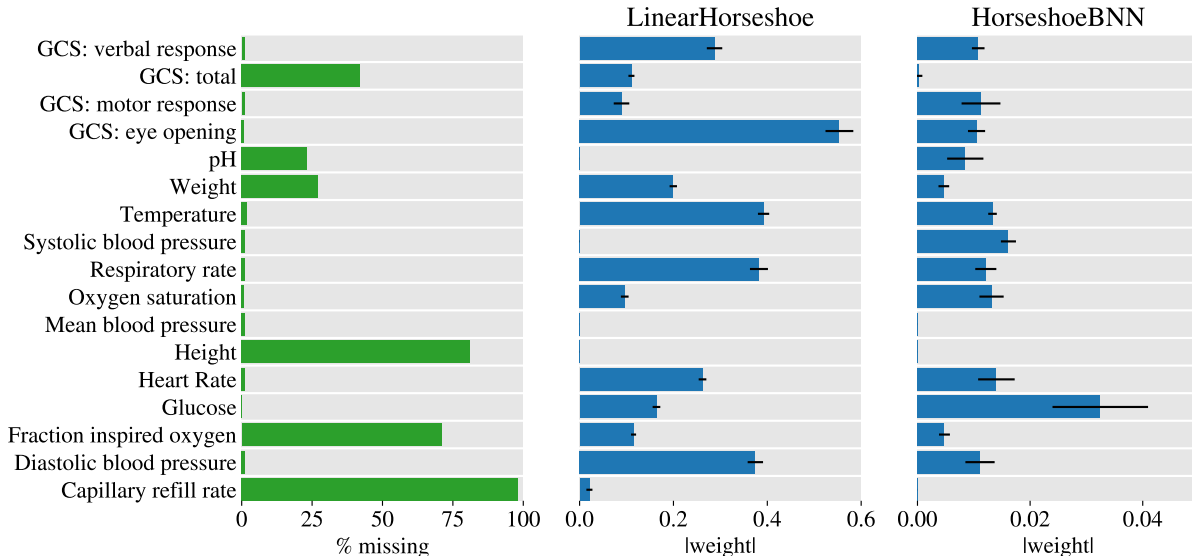


Figure 2: **Left:** percentage of missing data for the features in the MIMIC-III cohort. **Middle:** Norm of the weights of the LinearHorseshoe model, representing the relative importance of the corresponding features. **Right:** Norm of the weights of the HorseshoeBNN. The name of each input feature is given on the far left of the plots. Feature weights of zero indicate that the corresponding features are irrelevant for outcome prediction. All non-zero weights indicate that the corresponding features are relevant for predicting mortality.

the LinearHorseshoe model, but considered irrelevant by the HorseshoeBNN. Note the Glasgow coma total scale is the sum of the verbal response, motor response and eye opening, and the latter three features are all selected by the HorseshoeBNN.

Two features, namely *height* and *capillary refill rate* (*CRR*) are considered irrelevant by both models. While height is considered not informative by the domain expert, *CRR* is expected to be relevant. However, *CRR* is observed for an extremely small fraction of patients, which can explain why the model did not consider it.

Overall these results suggest that, compared to a linear model, a non-linear model like our HorseshoeBNN can provide additional insights into feature relevance.

Mortality prediction on CENTER-TBI

Cohort The CENTER-TBI (Collaborative European NeuroTrauma Effectiveness Research in Traumatic Brain Injury)

study is an observational study conducted across Europe and Israel (Maas et al. 2014). It contains data from 5400 patients with traumatic brain injury (TBI). We focus on the subset of patients in the emergency room and admitted to the ICU. The cohort contains a broad range of clinical data, including baseline demographics, mechanism of injury, vital signs, Glasgow coma scale, and brain computed tomographic reports and many other features.

Model	Error rate	AUROC	NLL
LinearGaussian	0.185 ± 0.008	0.871 ± 0.013	0.393 ± 0.018
GaussianBNN	0.195 ± 0.010	0.869 ± 0.013	0.390 ± 0.020
LinearHorseshoe	0.180 ± 0.008	0.874 ± 0.013	0.383 ± 0.016
HorseshoeBNN	0.179 ± 0.008	0.873 ± 0.013	0.380 ± 0.014
Lasso	0.192 ± 0.009	0.844 ± 0.013	0.423 ± 0.013
SVM	0.182 ± 0.007	-	-
RandomForest	0.182 ± 0.011	-	-

Table 4: Results of the different models for the task of mortality prediction tested on the CENTER-TBI cohort. NLL is the negative log-likelihood. The mean value and standard error of each metric over 10-fold cross-validation is presented.

Feature	Linear Horseshoe	Horseshoe BNN	IMPACT
Age	x	x	x
Sex	x	x	
Heart rate	x	x	
pH	x	x	
Hypoxia	x		x
Hypotension			x
GCS: motor response	x	x	x
Pupil reaction	x	x	x
Marshall CT Classification	x	x	x
Subarachnoid hemorrhage			x
Absent basal cisterns	x	x	
Extradural Hematoma	x	x	x
Glucose	x	x	x
Hemoglobin			x
International normalized ratio	x	x	
23 remaining features			

Table 5: List of features marked as relevant by the models. Features marked with an x are relevant.

Preprocessing We predict mortality based on the features listed in Table 9 of appendix D, using release 1.0 of the CENTER-TBI cohort. We remove the data of patients for which no outcome was reported. To address missing values we use zero-imputation for binary features and mean imputation for continuous and ordinal features, as suggested by clinicians. The final cohort contains 1613 samples and 38 features (see Appendix D). 75% of patients in the cohort survived, 25% deceased.

Prediction The results are summarized in Table 4 and confusion matrices are shown in Appendix D. We again observe that the HorseshoeBNN achieves slightly better performance than the linear models. The GaussianBNN performs worse than all other models. This could be due to the large amount of noise in the data which the GaussianBNN might be modeling, thereby overfitting the data. In contrast, the HorseshoeBNN removes input features which makes the model less likely to overfit.

Interpretability and Clinical Relevance The relevance of the input features as determined by the LinearHorseshoe model, the HorseshoeBNN and the RandomForest are shown in Figures 8 and 9 in Appendix D. Most of the weights of the RandomForest are similar, making this model unsuitable for feature selection. In Table 5 we compare the

features identified as relevant by the LinearHorseshoe model and the HorseshoeBNN. We also list features included in the IMPACT model (Steyerberg et al. 2008), a model commonly used for outcome prediction in TBI. We observe a large overlap between features used in the IMPACT model and features considered important by our horseshoe models, which is an indication that our feature selection method works correctly. The LinearHorseshoe model and the HorseshoeBNN attribute similar relevance to most features.

Interestingly, our models attribute little relevance to events of *hypotension*, although such events are considered important from a clinical perspective. A clinically likely explanation for this is that hypotension is typically unrecognized, leading to many false negatives for this feature.

Similar to hypotension, both models consider the feature *hemoglobin* irrelevant for mortality prediction. This might be explained by the small role of hemoglobin in the IMPACT model. It is also possible that the small effect of hemoglobin is already accounted for by the feature *international normalized ratio*. Furthermore, both models select certain features that are not part of the IMPACT model: *sex*, *heart rate*, *pH*, *international normalized ratio* and *absent basal cisterns*. In Appendix E we compare the feature relevance determined for the CENTER-TBI and the MIMIC-III datasets.

Conclusion and Future Work

We proposed a novel model, the HorseshoeBNN, for performing interpretable patient outcome prediction. Our method extends traditional BNNs to perform feature selection using sparsity inducing prior distributions in a tied manner. Our architecture offers many advantages. Firstly, being based on a BNN, it represents a non-linear, fully probabilistic method which is highly compatible with the clinical decision making process. Secondly, with our proposed advances, the model is able to learn which input features are important for prediction, thereby making it interpretable, which is highly desirable in the clinical domain.

We worked closely with clinicians and evaluated our model using two real-world ICU cohorts. We showed that our proposed HorseshoeBNN can provide additional insights about the importance of input features. Together with its ability to provide uncertainty estimates, the HorseshoeBNN could be used to support clinicians in their decision making process. In view of the high-dimensional complex nature of medical data and the high relevance of outcome prediction in healthcare, our method could be useful not only for ICUs but in any medical settings. Our work illustrates how a close collaboration between computational and clinical experts can lead to methodological advances suitable for translation into tools for patient benefit.

In future work, we will extend our model to be able to work with the entire time series (Yoon, Zame, and van der Schaar 2018) as dynamic prediction is a key area of interest in the ICU. Utilizing information about the evolution of features over time might not only improve predictive accuracy, but could provide additional insights about temporal changes of measurement values.

Moreover, we will use more sophisticated methods for missing value imputation to obtain better predictive perfor-

mance (Ma et al. 2019; Little and Rubin 2019). Finally, contemporary digital healthcare is fundamentally transdisciplinary and we would like to continue working with medical experts to explore how to deploy our method in a real-world clinical setting.

Acknowledgements

CENTER-TBI is supported by The European Union FP 7th Framework program (grant 602150) with additional funding provided by the Hannelore Kohl Foundation (Germany) and by the non-profit organization One Mind For Research (directly to INCF).

References

- [Beal 2003] Beal, M. J. 2003. *Variational algorithms for approximate Bayesian inference*. Ph.D. Dissertation, University of London.
- [Betancourt and Girolami 2015] Betancourt, M., and Girolami, M. 2015. Hamiltonian Monte Carlo for hierarchical models. In *Current trends in Bayesian methodology with applications*.
- [Bishop 2006] Bishop, C. M. 2006. *Pattern recognition and machine learning*. Springer.
- [Blundell et al. 2015] Blundell, C.; Cornebise, J.; Kavukcuoglu, K.; and Wierstra, D. 2015. Weight uncertainty in neural networks. *arXiv:1505.05424*.
- [Bojarski et al. 2016] Bojarski, M.; Del Testa, D.; Dworakowski, D.; Firner, B.; et al. 2016. End to end learning for self-driving cars. *arXiv:1604.07316*.
- [Boulanger-Lewandowski, Bengio, and Vincent 2012] Boulanger-Lewandowski, N.; Bengio, Y.; and Vincent, P. 2012. Modeling temporal dependencies in high-dimensional sequences: Application to polyphonic music generation and transcription. *arXiv:1206.6392*.
- [Bouton et al. 2016] Bouton, C.; Shaikhouni, A.; Annetta, N.; Bockbrader, M.; et al. 2016. Restoring cortical control of functional movement in a human with quadriplegia. *Nature* 533(7602).
- [Caballero B. and Akella 2015] Caballero B., K. L., and Akella, R. 2015. Dynamically modeling patient’s health state from electronic medical records: A time series approach. In *KDD Conference*. ACM.
- [Caruana et al. 2015] Caruana, R.; Lou, Y.; Gehrke, J.; Koch, P.; Sturm, M.; and Elhadad, N. 2015. Intelligible models for healthcare: Predicting pneumonia risk and hospital 30-day readmission. In *SIGKDD*. ACM.
- [Carvalho, Polson, and Scott 2009] Carvalho, C.; Polson, N.; and Scott, J. 2009. Handling sparsity via the horseshoe. In *AISTATS*.
- [Celi et al. 2012] Celi, L.; Galvin, S.; Davidzon, G.; Lee, J.; Scott, D.; and Mark, R. 2012. A database-driven decision support system: customized mortality prediction. *Journal of personalized medicine* 2(4).
- [Che et al. 2018] Che, Z.; Purushotham, S.; Cho, K. N.; Sontag, D.; and Liu, Y. 2018. Recurrent neural networks for multivariate time series with missing values. *Sci. Rep.* 8(1).
- [Chen et al. 2017] Chen, M.; Hao, Y.; Hwang, K.; Wang, L.; and Wang, L. 2017. Disease prediction by machine learning over big data from healthcare communities. *IEEE Access* 5.
- [Collobert et al. 2011] Collobert, R.; Weston, J.; Bottou, L.; Karlen, M.; Kavukcuoglu, K.; and Kuksa, P. 2011. Natural language processing (almost) from scratch. *J. Mach. Learn. Res.* 12(Aug).
- [Elixhauser et al. 1998] Elixhauser, A.; Steiner, C.; Harris, D. R.; and Coffey, R. M. 1998. Comorbidity measures for use with administrative data. *Medical care* 8–27.
- [Ghassemi et al. 2014] Ghassemi, M.; Naumann, T.; Doshi-Velez, F.; Brimmer, N.; Joshi, R.; Rumshisky, A.; and Szolovits, P. 2014. Unfolding physiological state: Mortality modelling in intensive care units. In *KDD Conference*.
- [Ghosh and Doshi-Velez 2017] Ghosh, S., and Doshi-Velez, F. 2017. Model selection in Bayesian neural networks via horseshoe priors. *arXiv:1705.10388*.
- [Harutyunyan et al. 2017] Harutyunyan, H.; Khachatrian, H.; Kale, D.; and Galstyan, A. 2017. Multitask learning and benchmarking with clinical time series data. *arXiv:1703.07771*.
- [Hernández-Lobato and Adams 2015] Hernández-Lobato, J. M., and Adams, R. 2015. Probabilistic backpropagation for scalable learning of Bayesian neural networks. In *ICML*.
- [Hernández-Lobato, Hernández-Lobato, and Suárez 2015] Hernández-Lobato, J. M.; Hernández-Lobato, D.; and Suárez, A. 2015. Expectation propagation in linear regression models with spike-and-slab priors. *Machine Learning* 99(3).
- [Hinton and Van Camp 1993] Hinton, G. E., and Van Camp, D. 1993. Keeping the neural networks simple by minimizing the description length of the weights. In *COLT*.
- [Ingraham and Marks 2016] Ingraham, J. B., and Marks, D. S. 2016. Bayesian sparsity for intractable distributions. *arXiv:1602.03807*.
- [Johnson et al. 2016] Johnson, A. E.; Pollard, T. J.; Shen, L.; Lehman, L. W.; Feng, M.; Ghassemi, M.; Moody, B.; Szolovits, P.; Celi, L. A.; and Mark, R. G. 2016. MIMIC-III, a freely accessible critical care database. *Sci Data* 3.
- [Jordan et al. 1999] Jordan, M. I.; Ghahramani, Z.; Jaakkola, T. S.; and Saul, L. K. 1999. An introduction to variational methods for graphical models. *Machine learning* 37(2).
- [Joshi and Szolovits 2012] Joshi, R., and Szolovits, P. 2012. Prognostic physiology: modeling patient severity in intensive care units using radial domain folding. In *AMIA Annual Symposium Proceedings*, volume 2012.
- [Kingma and Ba 2014] Kingma, D. P., and Ba, J. 2014. Adam: A method for stochastic optimization. *arXiv:1412.6980*.
- [Kingma and Welling 2013] Kingma, D. P., and Welling, M. 2013. Auto-encoding variational Bayes. *arXiv:1312.6114*.
- [Knaus et al. 1985] Knaus, W. A.; Draper, E. A.; Wagner, D. P.; and Zimmerman, J. E. 1985. APACHE II: a severity of disease classification system. *Crit. Care Med.* 13(10).
- [Le Gall, Lemeshow, and Saulnier 1993] Le Gall, J.; Lemeshow, S.; and Saulnier, F. 1993. A new simplified acute physiology score (SAPS II) based on a european/north american multicenter study. *Jama* 270(24).
- [Lemeshow et al. 1993] Lemeshow, S.; Teres, D.; Klar, J.; Avrunin, J. S.; Gehlbach, S. H.; and Rapoport, J. 1993. Mortality probability models based on an international cohort of intensive care unit patients. *Jama* 270(20).
- [Little and Rubin 2019] Little, R. J. A., and Rubin, D. B. 2019. *Statistical analysis with missing data*. Wiley.
- [Louizos, Ullrich, and Welling 2017] Louizos, C.; Ullrich, K.; and Welling, M. 2017. Bayesian compression for deep learning. In *NeurIPS*.
- [Ma et al. 2019] Ma, C.; Tschitschek, S.; Palla, K.; Hernández-Lobato, J. M.; Nowozin, S.; and Zhang, C. 2019. Eddi: Efficient dynamic discovery of high-value information with partial VAE. In *ICML*.
- [Maas et al. 2014] Maas, A. I. R.; Menon, D. K.; Steyerberg, E. W.; Citerio, G.; Lecky, F.; Manley, G. T.; Hill, S.; Legrand, V.; and Sorgner, A. 2014. Collaborative european neurotrauma effectiveness research in traumatic brain injury (center-tbi) a prospective longitudinal observational study. *Neurosurgery* 76(1).

- [MacKay and others 1994] MacKay, D. J. C., et al. 1994. Bayesian nonlinear modeling for the prediction competition. *ASHRAE transactions* 100(2).
- [MacKay 1992] MacKay, D. J. C. 1992. A practical Bayesian framework for backpropagation networks. *Neural Computation* 4(3).
- [Meiring et al. 2018] Meiring, C.; Dixit, A.; Harris, S.; MacCallum, N. S.; Brealey, D. A.; Watkinson, P. J.; Jones, A.; Ashworth, S.; Beale, R.; Brett, S. J.; Singer, M.; and Ercole, A. 2018. Optimal intensive care outcome prediction over time using machine learning. *PLoS ONE* 13(11).
- [Mitchell and Beauchamp 1988] Mitchell, T., and Beauchamp, J. 1988. Bayesian variable selection in linear regression. *JASA* 83(404).
- [Park and Casella 2008] Park, T., and Casella, G. 2008. The Bayesian lasso. *JASA* 103(482).
- [Ranganath, Gerrish, and Blei 2014] Ranganath, R.; Gerrish, S.; and Blei, D. 2014. Black box variational inference. In *AISTATS*.
- [Rezende, Mohamed, and Wierstra 2014] Rezende, D. J.; Mohamed, S.; and Wierstra, D. 2014. Stochastic backpropagation and approximate inference in deep generative models. In *ICML*.
- [Shipp et al. 2002] Shipp, M.; Ross, K.; Tamayo, P.; Weng, A.; et al. 2002. Diffuse large b-cell lymphoma outcome prediction by gene-expression profiling and supervised machine learning. *Nature medicine* 8(1).
- [Silver et al. 2016] Silver, D.; Huang, A.; Maddison, C.; Guez, A.; et al. 2016. Mastering the game of go with deep neural networks and tree search. *Nature* 529(7587).
- [Steyerberg et al. 2008] Steyerberg, E. W.; Mushkudiani, N.; Perel, P.; Butcher, I.; et al. 2008. Predicting outcome after traumatic brain injury: development and international validation of prognostic scores based on admission characteristics. *PLoS medicine* 5(8).
- [Tibshirani 1996] Tibshirani, R. 1996. Regression shrinkage and selection via the Lasso. *J. Royal Stat. Soc.: B* 58(1).
- [Yoon, Zame, and van der Schaar 2018] Yoon, J.; Zame, W. R.; and van der Schaar, M. 2018. Deep sensing: Active sensing using multi-directional recurrent neural networks. In *ICLR*.
- [Zhang et al. 2018] Zhang, C.; Butepage, J.; Kjellstrom, H.; and Mandt, S. 2018. Advances in variational inference. *IEEE TPAMI*.

A Validation of Induced Sparsity

In this section, we verify the sparsity-inducing capacities of our LinearHorseshoe model. We repeat an experiment proposed in (Hernández-Lobato, Hernández-Lobato, and Suárez 2015). In the experiment, a data matrix X with 75 datapoints is sampled from the unit hypersphere. Target values y are computed using $y = X \cdot w + \epsilon$, where ϵ represents Gaussian distributed noise with standard deviation 0.005. The 512-dimensional weight vector w is sparse, that is, only 20 randomly selected components are non-zero.

Because the target values y depend linearly on the data matrix X , we use a linear model with a horseshoe prior to obtain an estimate \tilde{w} of the weight vector. The estimate \tilde{w} is given by the mean of the posterior distribution. We evaluate the model using the reconstruction error $\|\tilde{w} - w\|/\|w\|$ and find results similar to those reported in (Hernández-Lobato, Hernández-Lobato, and Suárez 2015). Hyperparameter settings can be found in Table 6. The results of this validation experiment show that our model is capable of correctly reproducing sparse weight vectors.

Hyperparameter	Value
Number of weight samples during training	10
Number of weight samples during testing	100
Batch size	64
Learning rate	0.001
Number of epochs	2000000
Global shrinkage parameter b_g of Horseshoe prior	1.0
Local shrinkage parameter b_0 of Horseshoe prior	1.0

Table 6: Parameter and hyperparameter settings for prior experiment on induced sparsity

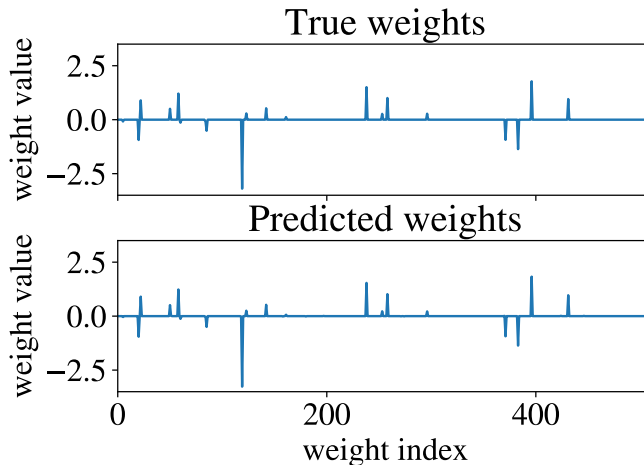


Figure 3: Signal reconstruction (bottom) of a sparse signal (top).

The average reconstruction error over twenty realizations of the experiment is 0.399 ± 0.272 . This error is slightly higher but of the same order of magnitude as the error of 0.16 ± 0.07 reported in (Hernández-Lobato, Hernández-Lobato, and Suárez 2015). The difference can be explained by the fact that we use variational inference to approximate the posterior distribution whereas (Hernández-Lobato, Hernández-Lobato, and Suárez 2015) use Markov chain Monte Carlo techniques, which are known to give a more accurate approximation of the posterior distribution. An example of a sparse signal and the reconstructed weights is shown in Figure 3.

B Models

For the comparison with existing models, we make use of feature selection models implemented in *Scikit Learn*. For the benchmarking on regression datasets from the UCI repository, we compare to the *Lasso* model, the *SVR* model (a support vector regressor) with linear kernel and the *RandomForestRegressor*. For classification tasks we use the *LogisticRegression* model with ℓ_1 regularization (equivalent to Lasso), the *LinearSVC* model with ℓ_1 regularization and the *RandomForestClassifier*. For all models the regularization strength is optimized to minimize the test error.

C MIMIC-III

C.1 Feature ranges and hyperparameters

Allowed ranges for the features in the MIMIC-III dataset are shown in Table 7. Table 8 shows the hyperparameters for the horseshoeBNN.

Feature	Unit	Min thresh-old	Max thresh-old
Height	cm	> 0	250
Temperature	°C	20	49
Blood pH*	-	6	8
Fraction of inspired oxygen	-	0	1
Capillary refill time	seconds	0	-
Heart rate	bpm	0	300
Systolic blood pressure	mmHg	> 0	275
Diastolic blood pressure	mmHg	> 0	150
Mean blood pressure	mmHg	> 0	190
Weight	kg	0	250
Glucose	mg/dL	0	1250
Respiratory rate	number breaths per min	0	150
Oxygen saturation	%	> 0	100
Glasgow coma scale eye response	-	1	4
Glasgow coma scale motor response	-	1	6
Glasgow coma scale verbal response	-	1	5
Glasgow coma scale total	-	3	15

Table 7: MIMIC-III feature ranges *For blood pH values higher than 14 (physically impossible), we assume that these are actually measures of hydrogen ion concentrations in nanomole/L. These values are converted to pH values, after which the threshold is applied.

Hyperparameter	Value
Number of weight samples during training	10
Number of weight samples during testing	100
Batch size	64
Number of hidden units	50
Learning rate	0.001
Number of epochs	5000
Standard deviation of Gaussian prior	1.0
Global shrinkage parameter b_g of Horseshoe prior	1.0
Local shrinkage parameter b_0 of Horseshoe prior	1.0

Table 8: Parameter and hyperparameter settings for MIMIC models

C.2 Confusion matrices

Figure 4 shows the confusion matrices for the models trained on the MIMIC-III dataset.

C.3 Weight histograms

We inspect the histograms of the means of the distributions of the weights of the LinearHorseshoe and LinearGaussian models. For the GaussianBNN and the HorseshoeBNN, we calculate the average weight per feature in the first layer. These weights are shown in the histograms in Fig. 5 The histograms corresponding to the LinearHorseshoe model and the HorseshoeBNN models show a clearer separation into two groups (see red dotted lines): the irrelevant weights shrink more because of the horseshoe prior. This demonstrates that models with a horseshoe prior are better suited for feature selection than models with Gaussian priors.

C.4 Alternative threshold determination

The importance of the j th feature can also be determined by inspecting the posterior distribution of the scale parameters v and τ_j . As can be seen in Equation 10, the product $v\tau_j$ follows a log-normal distribution. Louizos, Ullrich, and Welling (2017)

	LinearGaussian		GaussianBNN		LinearHorseshoe		HorseshoeBNN	
True label survived	0.979	0.021	0.975	0.021	0.979	0.021	0.975	0.025
	±	±	±	±	±	±	±	±
True label deceased	0.001	0.001	0.002	0.002	0.001	0.001	0.003	0.003
	±	±	±	±	±	±	±	±
survived	0.819	0.181	0.743	0.257	0.825	0.175	0.743	0.257
	±	±	±	±	±	±	±	±
deceased	0.008	0.008	0.015	0.015	0.008	0.008	0.018	0.018
	±	±	±	±	±	±	±	±
	Predicted label		Predicted label		Predicted label		Predicted label	

Figure 4: Results of the different models for the task of mortality prediction tested on the MIMIC-III cohort. The mean value and one standard error of each metric over 10-fold cross-validation is presented.

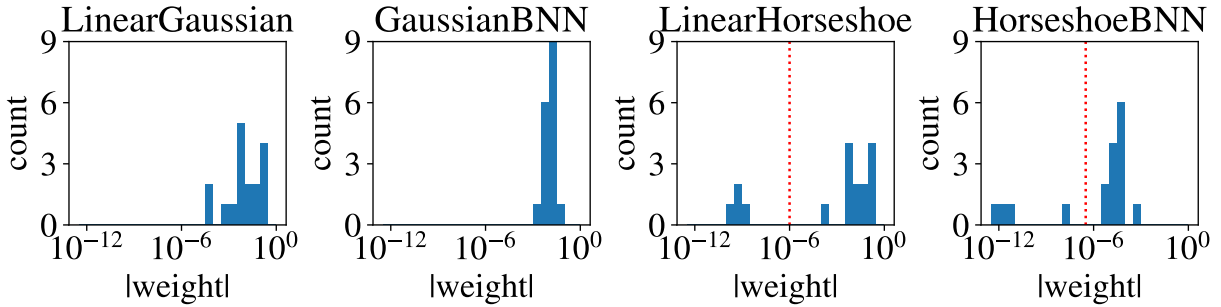


Figure 5: Histograms of the weights of the first layers of the models. Horseshoe models show more significant shrinkage of irrelevant weights.

determine relevance by setting a threshold for the mode of this distribution. The modes of the posterior distributions of $v\tau_j$ for the features as determined by the LinearHorseshoe model are shown in Fig. 6. The features left of the dotted threshold line (*Height, Mean blood pressure, Systolic blood pressure* and *pH*) are considered irrelevant by the model. This is in agreement with the findings in Fig. 2 in the main text. Figure 6 shows a similar result for the mode of the posterior distribution of $v\tau_j$ for the HorseshoeBNN. Again, the features considered irrelevant are the same as in Fig. 2.

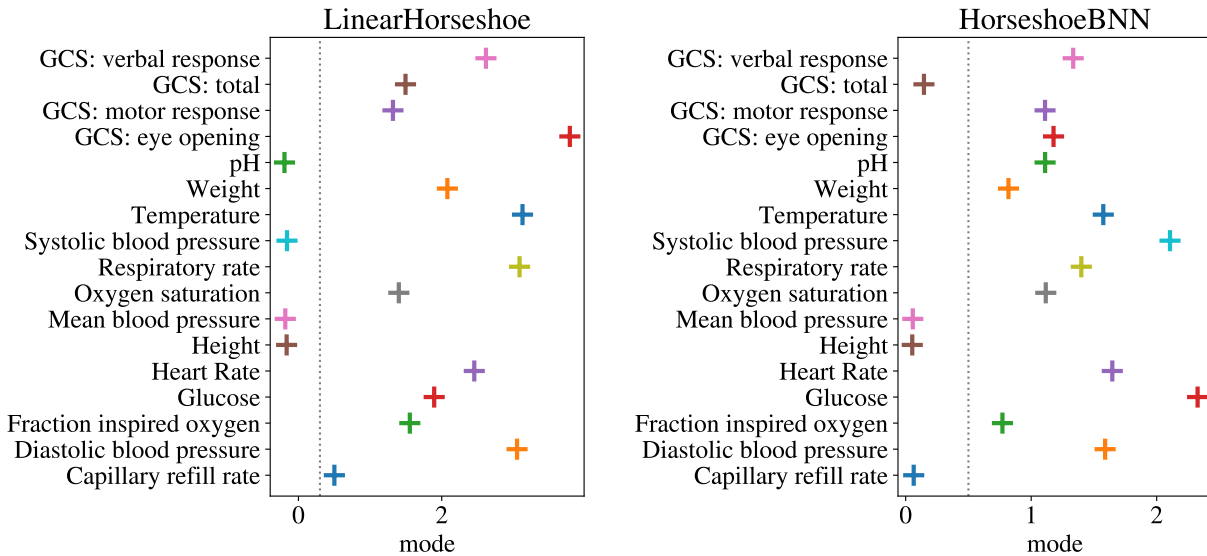


Figure 6: Mode of the posterior distribution of $v\tau_j$ for all features j as determined by the LinearHorseshoe model (left) and the HorseshoeBNN (right). The dotted line indicates the threshold for feature relevance.

D CENTER-TBI

D.1 Feature ranges and hyperparameters

The features in the CENTER-TBI dataset are listed in Table 9. Table 10 shows the hyperparameters for the horseshoeBNN.

Category	Features
General	Age, gender, prior alcohol use, history of anti-coagulants
Injury	Cause of injury, time of injury
Condition on arrival	heart rate, respiratory rate, temperature, SpO ₂ Systolic blood pressure, diastolic blood pressure Arterial O ₂ tension, CO ₂ tension, pH Assessment of airway, breathing, circulation Episode of hypoxia or hypotension
Neurological assessment	Glasgow Coma Score, pupil reaction
Initial imaging	Marshall classification, depressed skull fracture subarachnoid hemorrhage, midline shift Absent basal cisterns, extradural hematoma
Blood chemistry tests	Glucose, sodium, albumin, calcium, hemoglobin hematocrit, white blood cell count, C-reactive protein, Platelet count, International normalized ratio activated partial thromboplastin time, fibrogen

Table 9: Features used to predict mortality on the CENTER-TBI dataset

Hyperparameter	Value
Number of weight samples during training	10
Number of weight samples during testing	100
Batch size	64
Number of hidden units	100
Learning rate	0.001
Number of epochs	5000
Standard deviation of Gaussian prior	1.0
Global shrinkage parameter b_g of Horseshoe prior	1.0
Local shrinkage parameter b_0 of Horseshoe prior	1.0

Table 10: Parameter and hyperparameter settings for CENTER-TBI models

D.2 Confusion matrices

Figure 7 shows the confusion matrices for the models trained on the CENTER-TBI dataset. Just as for the MIMIC-III dataset, the BNN based models are better at predicting the outcome for deceased patients than the linear models.

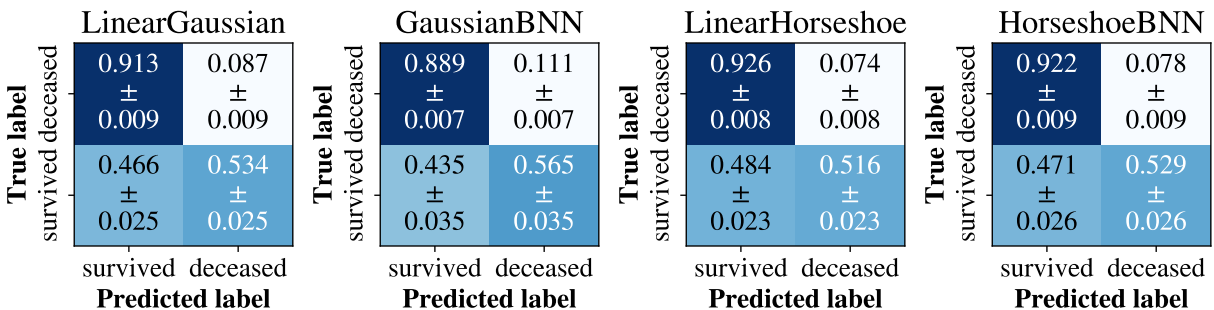


Figure 7: Results of the different models for the task of mortality prediction tested on the CENTER-TBI cohort. The mean value and one standard error of each metric over 10-fold cross-validation is presented.

D.3 Feature importance

The full graph of the relevance of the different input features as determined by the LinearHorseshoe model and the HorseshoeBNN are shown in Figure 8. Features marked in bold are included in the IMPACT model (Steyerberg et al. 2008), a model commonly used for outcome prediction in TBI.

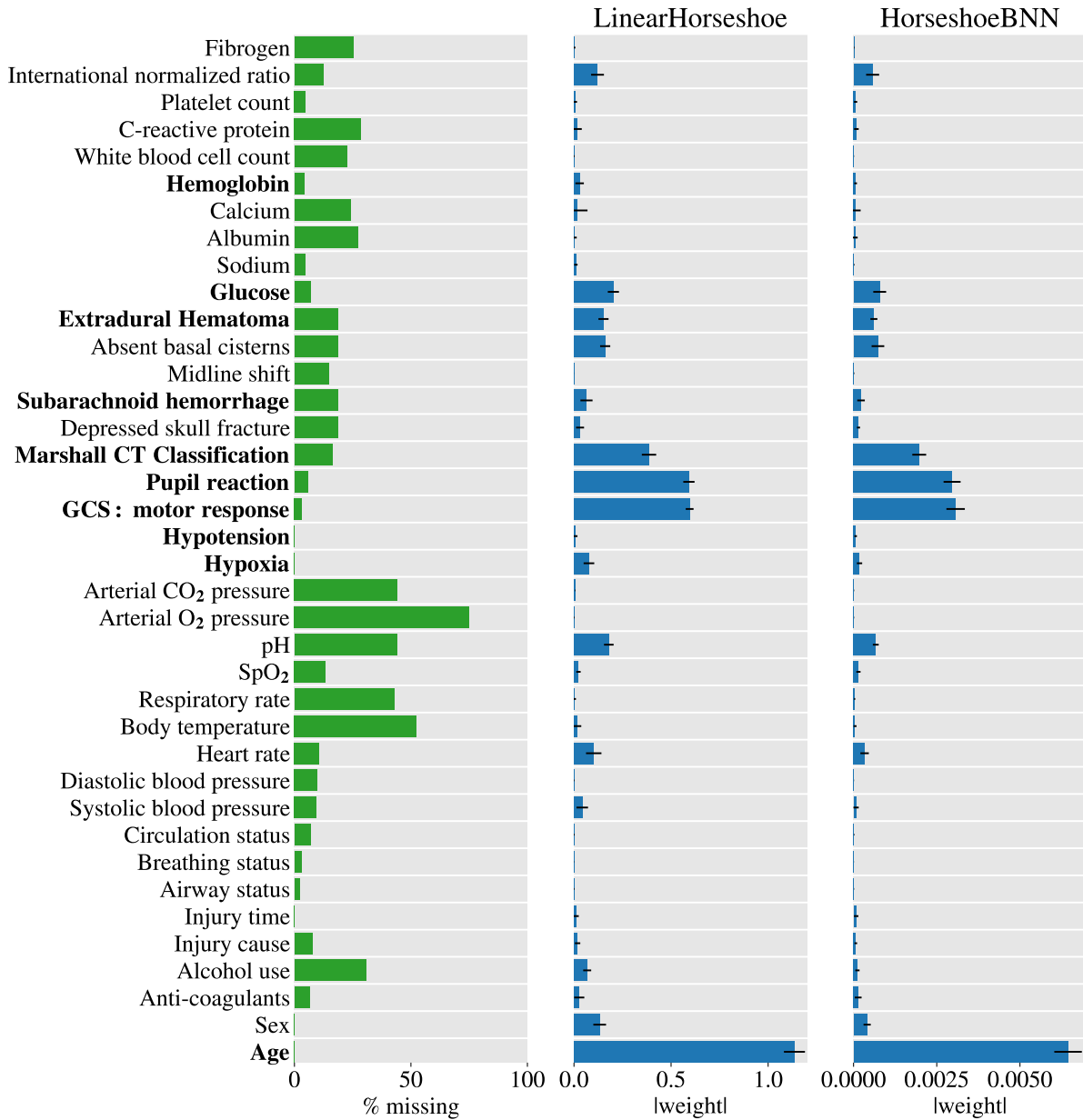


Figure 8: **Left:** Percentage of missing data for the features in the CENTER-TBI cohort. **Middle:** Norm of the weights of the LinearHorseshoe model, representing the relative importance of the corresponding features. **Right:** Norm of the weights of the HorseshoeBNN. The name of each input feature is given on the far left of the plots. Features included in the IMPACT model for outcome prediction in TBI are marked bold. Feature weights of zero indicate that the corresponding features are irrelevant for outcome prediction. All non-zero weights indicate that the corresponding features are relevant for predicting mortality.

D.4 Feature importance - RandomForest

Figure 9 compares the relevance of features attributed by the RandomForest and the HorseshoeBNN. The models agree on the four most important features, but for the RandomForest all other weights are roughly equal in size. It is therefore unable to

distinguish other relevant features.

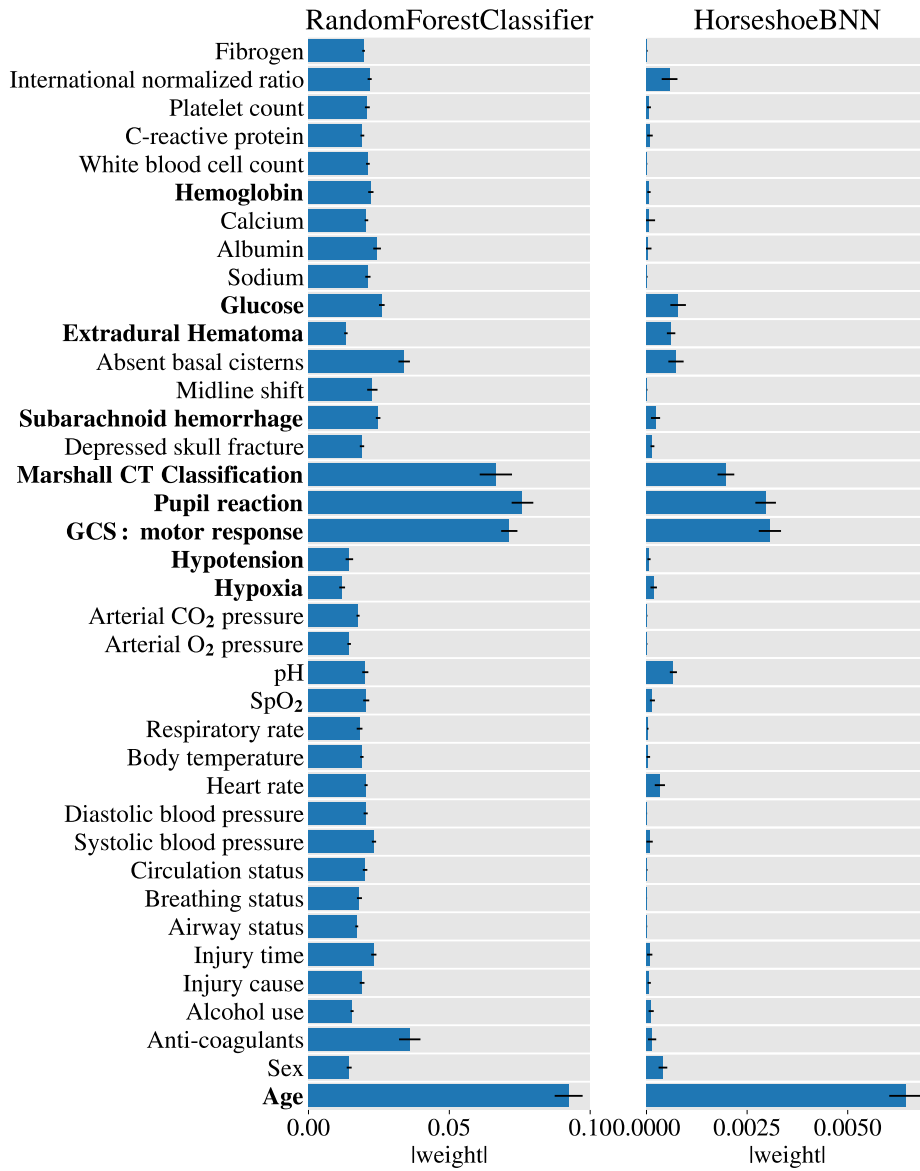


Figure 9: **Left:** Norm of the weights of the RandomForest **Right:** Norm of the weights of the HorseshoeBNN.

E Discussion of feature selection results

When comparing with the results for MIMIC-III we observe different results for the feature pH . Whereas both horseshoe models trained on CENTER-TBI determine pH to be important, this is not the case for MIMIC-III. For the latter only the non-linear model, that is, the HorseshoeBNN, selects this feature. This may be due to a difference between the patient groups contained in MIMIC-III and CENTER-TBI. This assumption is further supported by the distribution of pH values in the cohorts. This can be explained by the difference between the patient groups contained in MIMIC vs. CENTER-TBI. Whereas MIMIC contains a very heterogeneous group of patients, CENTER-TBI contains only patients that experienced some kind of trauma, and the outcome predictors will therefore be expected to be very different given this is a different disease. Figure 10 illustrates the distribution of pH in both datasets. When computing the KL-divergence between the distributions for patients that survived and patients that deceased we observe that the divergence is larger for CENTER-TBI. This might explain why both models determine pH to be important for CENTER-TBI, whereas only the non-linear model includes pH for MIMIC.

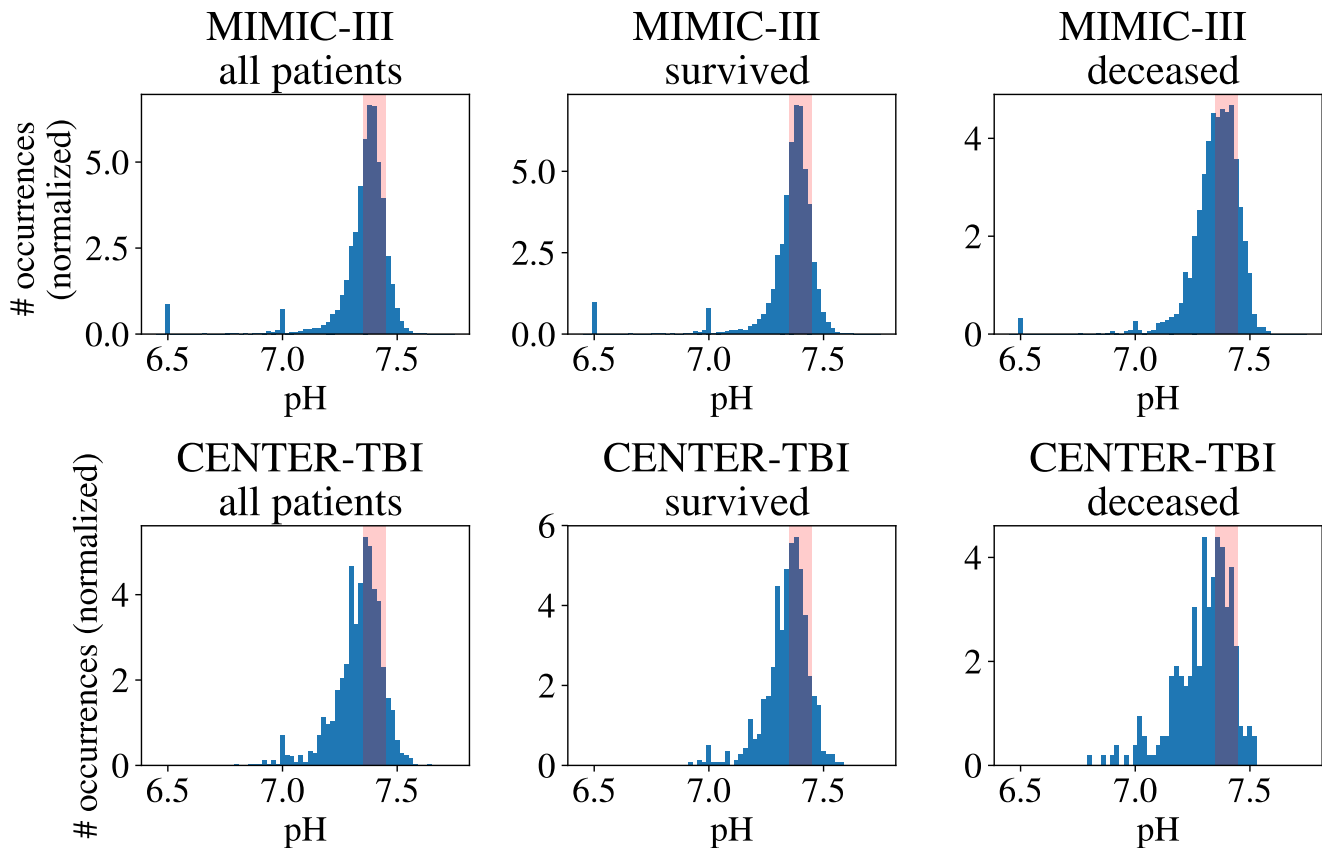


Figure 10: Distribution of the feature pH in the MIMIC and CENTER-TBI cohorts. Illustrated in red is the range of pH for healthy patients (7.35-7.45).

A further difference was observed for blood pressure. Both CENTER-TBI horseshoe models indicate that only systolic blood pressure is of relevance, whereas for MIMIC-III the HorseshoeBNN determined both systolic and diastolic blood pressure to be important. Again, this could be explained by the heterogeneity of the datasets. CENTER-TBI contains predominantly people with relatively isolated brain injuries not affecting the blood circulation. Therefore, blood pressure (absolute, e.g. systolic) is most important as this pressure perfuses the brain. In contrast, MIMIC-III includes a large number of patients in shock (e.g. with sepsis). The degree of this pathology, which would be less likely to occur in the CENTER-TBI patients, is clinically likely to be a strong determinant of outcome and would be expected to be reflected in a difference in diastolic blood pressure. This is further supported when inspecting the relationship between systolic and diastolic blood pressure in both datasets. Figure 11 shows that the two features are strongly correlated for CENTER-TBI but not for MIMIC. This might explain why only the systolic blood pressure is considered relevant for CENTER-TBI, but both the systolic and diastolic blood pressure for MIMIC.

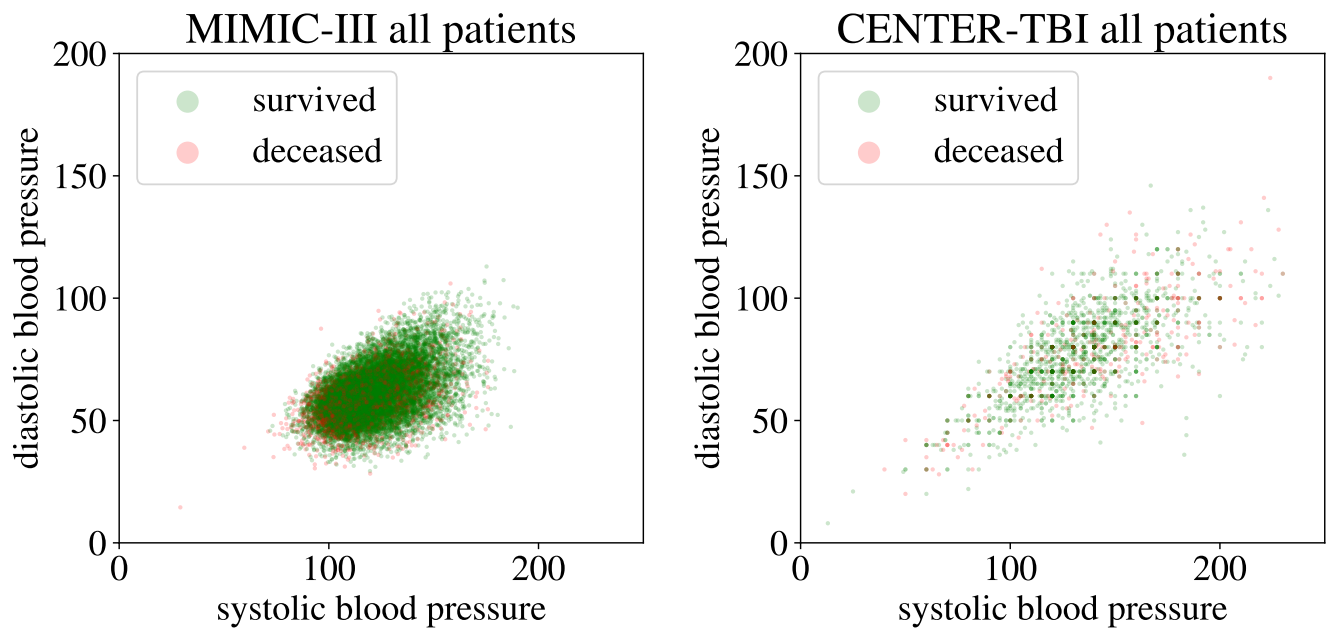


Figure 11: Correlations between the features *diastolic blood pressure* and *systolic blood pressure* in the MIMIC and CENTER-TBI cohorts.